AIAA 80-1668R

Control of a Large Flexible Platform in Orbit

A.S.S.R. Reddy,* P.M. Bainum,† and R. Krishna‡
Howard University, Washington, D.C.
and H.A. Hamer§
NASA Langley Research Center, Hampton, Va.

The dynamics and attitude and shape control of a large, thin, flexible platform in orbit are studied. Attitude and shape control are assumed to result from actuators placed perpendicular to the main surface and one edge, and their effect on the rigid body and elastic modes is modeled to first order. The equations of motion are linearized about nominal orientations, where the undeformed plate follows either the local vertical or local horizontal. The stability of the uncontrolled system is investigated analytically. Once controllability is established for a set of actuator locations, control law development is based on pole placement, decoupling, and linear optimal control theory.

Nomenclature

A_r	= rth modal amplitude function
B	= control influence matrix
C_x, C_y, C_z	= disturbance torques about the principal undeformed body axes
E_r	= generic force on rth mode
f	= force due to an actuator
f_x, f_y, f_z	= force components due to an actuator
$G_{R_x}, G_{R_y}, G_{R_z}$	= gravity gradient torques about the principal undeformed body axes
I_x, I_y, I_z	= moments of inertia about the principal axes
K	= gain matrix
K_r, K_p	= rate and position feedback gain matrices
M_r	= rth modal mass
T	= torque due to an actuator
T_x, T_y, T_z	= torque components
$W_r(x,y)$	= rth modal shape function
Z_r	= nondimensionalized rth modal amplitude function
ω_c	= orbital frequency
$\omega_x, \omega_y, \omega_z$	= angular body rates
ϕ, ψ, θ	= roll, yaw, and pitch, respectively
$\omega_1, \omega_2, \omega_3$	= first three modal frequencies of the plate

I. Introduction

LARGE, flexible spacecraft systems have been proposed for future applications in widespread communications, electronic orbitally based mail systems, and as possible collectors of solar energy for transmittal to Earth-based receiving stations.[1,2] For such missions the size of the orbiting system may be several times larger than that of the Earth-based receiving station(s), and both orientation and shape control of the orbiting system will be required.

In order to gain insight into the dynamics of such a large, flexible system, the equations of motion of a long, flexible free-free beam in orbit were developed[3] using a slightly modified version of the general formulation of the dynamics of a general flexible orbiting body formulated by Santini.[4] This specific example considered only the in-plane rotations and deformations of the uncontrolled beam and demonstrated the possibility of instability for very small values of the ratio of the fundamental flexural frequency to the orbital angular velocity.

Two related papers treated the modeling of point actuators located at specific points along the beam with the associated criteria for controllability[5] and also the problem of selecting control law feedback gains based on decoupling techniques and application of the linear regulator problem.[6] Also included were numerical results showing the effects of control spillover on the uncontrolled modes when the number of controllers is less than the number of modes in the model, and the effects of inaccurate knowledge of the control influence coefficients which lead to errors in the calculated feedback gains.[6]

In the present paper the two-dimensional model considered in Refs. 3, 5, and 6 is extended to three dimensions by developing the equations of motion for a large, flexible rectangular plate (platform) in orbit. These equations include three rotational equations plus the generic mode elastic equations.

II. Model Development

In the present paper the following three different nominal orientations of the platform in orbit are assumed about which attitude and shape control are to be achieved.

Case 1: the platform following the local vertical with its larger surface perpendicular to the plane of the orbit (Fig. 1a).

Case 2: the platform following the local horizontal with its larger surface area normal to the local vertical (Fig. 1b).

Case 3: the platform following the local vertical with its larger surface perpendicular to the orbit normal (Fig. 1c).

From the general formulation of Refs. 3 and 4, the equations of motion of the structure are obtained, under the assumption that the structural transverse deformations are small compared to the characteristic length of the plate and also utilizing the (assumed) symmetry properties of the plate. Also included are the first-order gravity-gradient effects.[3,4]

A. Linearized Equations of Motion

With the further assumption of small-amplitude motion in the rigid modes, the rotational equations of motion can be

Presented as Paper 80-1668 at the AIAA/AAS Astrodynamics Conference, Danvers, Mass., Aug. 11-13, 1980; submitted Oct. 6, 1980; revision received March 27, 1981.

*Graduate Research Assistant, Dept. of Mechanical Eng.
†Professor of Aerospace Eng., Associate Fellow AIAA.
‡Graduate Research Assistant, Dept. of Mechanical Eng.
§Aerospace Technologist, Flight Dynamics and Control Division.

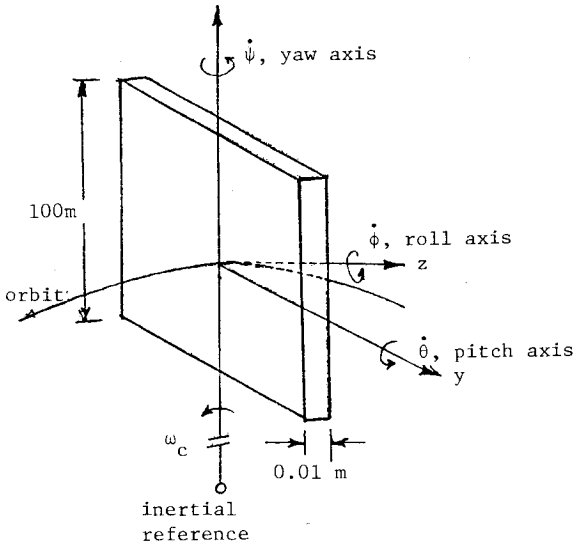

Fig. 1a Case 1—platform following the local vertical with major surface normal to the orbit plane.

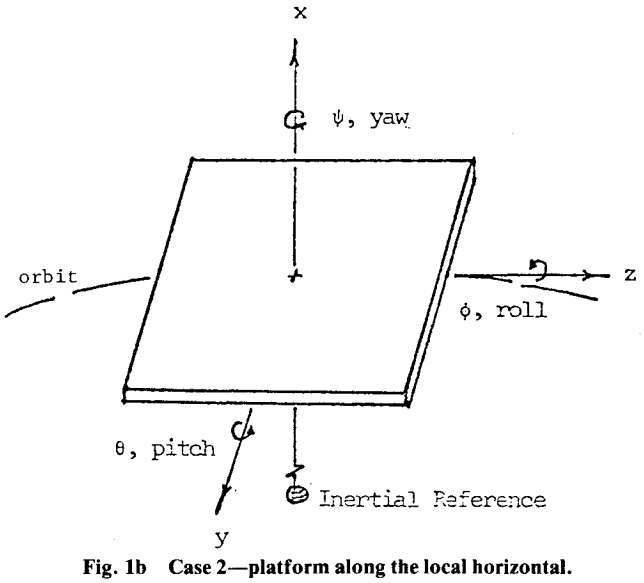

Fig. 1b Case 2—platform along the local horizontal.

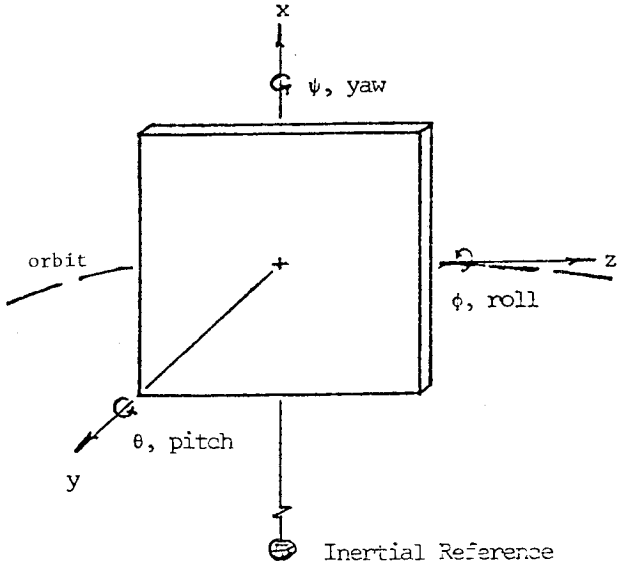

Fig. 1c Case 3—platform following the local vertical with major surface in the orbit plane.

developed to yield[7]

$$\ddot{\psi}=\omega_c\dot{\phi}\left[\frac{I_y-I_z}{I_x}-1\right]-\omega_c^2\left(\frac{I_y-I_z}{I_x}\right)\psi+\frac{T_x}{I_x}+\frac{C_x}{I_x}$$

$$\ddot{\phi}=\omega_c\dot{\psi}\left[\frac{I_x-I_y}{I_z}+1\right]+4\omega_c^2\left(\frac{I_x-I_y}{I_z}\right)\phi+\frac{T_z}{T_z}+\frac{C_z}{I_z}$$

$$\ddot{\theta}=3\omega_c^2\left(\frac{I_x-I_z}{I_y}\right)\theta+\frac{T_y}{I_y}+\frac{C_y}{I_y} \tag{1}$$

For the present analysis, the platform is assumed to be square, thin, and homogeneous, such that the following relationships among the principal moments of inertia are valid:

$$\begin{aligned}&\text{Case 1:}\quad I_x=I_y \text{ and } I_z=2I_x=2I_y\\ &\text{Case 2:}\quad I_y=I_z \text{ and } I_x=2I_y=2I_z\\ &\text{Case 3:}\quad I_x=I_z \text{ and } I_y=2I_x=2I_z\end{aligned} \tag{2}$$

The corresponding linearized form of the generic mode equations in terms of the flexural modal amplitudes[3,4] become

$$\begin{aligned}&\text{Case 1:}\quad \ddot{A}_r+\omega_r^2A_r=E_r/M_r\\ &\text{Case 2:}\quad \ddot{A}_r+(\omega_r^2-3\omega_c^2)A_r=E_r/M_r\\ &\text{Case 3:}\quad \ddot{A}_r+(\omega_r^2-\omega_c^2)A_r=E_r/M_r\end{aligned} \tag{3}$$

B. Modeling of Point Actuators

For an actuator which can generate a force of the type

$$\bar{f}=f_x\hat{i}+f_y\hat{j}+f_z\hat{k} \tag{4}$$

and placed at a location (x,y,z), the resultant control torque is given by

$$\bar{T}=\bar{R}\times\bar{f} \tag{5}$$

where $\bar{R}=x\hat{i}+y\hat{j}+z\hat{k}$ describes the position of the actuator on the surface (or edge) of the plate. Actuators can be placed perpendicular to the XY, YZ, or XZ planes of the plate, for example, for an actuator whose force axis is perpendicular to the XY plane the torque is given by (since $f_x=f_y=0$)

$$\bar{T}=yf_z\hat{i}-xf_z\hat{j} \tag{6}$$

The generic force due to the lth actuator on the rth mode is given by[3,4]

$$E_r=\iint W_r(x,y)\hat{k}\cdot\delta(x-x_l,y-y_l)f_l(t)\hat{k}\,dx\,dy$$

$$=W_r(x_l,y_l)f_l(t) \tag{7}$$

where $W_r(x,y)$ is the rth modal (spatial) function of the deformed plate with vibrations assumed to occur along the Z direction, whose amplitudes are assumed to be much smaller than a characteristic plate length.

For n actuators placed on the XY plane of the plate with force axes normal to that deformed surface, the generic force on the rth mode is given by

$$E_r=\sum_{i=1}^{n}W_r(x_i,y_i)f_i \tag{8}$$

where x_i,y_i are the coordinates of the ith actuator. An actuator placed normal to the X,Y plane will not produce a torque about the Z axis; in order to obtain a direct torque about the Z axis, actuators may have to be located on the other surfaces (edges) of the plate, and are also modeled in this paper.

The modeling of actuators that produce force components that are both spatially and time dependent (distributed actuators) is considered in Ref. 7.

III. Uncontrolled Motion—Numerical Example

The platform is assumed to have the following physical properties:

$a = 100$ m (side of square plate)

Mass, $M = 276{,}800$ kg

Minimum moment of inertia $= 2.354 \times 10^7$ kg-m^2

Maximum moment of inertia $= 4.7088 \times 10^7$ kg-m^2

For an assumed orbital altitude of 250 n.mi. (circular)

$$\omega_c = 1.25 \times 10^{-3} \text{ rad/s}$$

The modal frequencies of the elastic modes have been obtained using a finite-element computer algorithm.[7] For the first three flexible modes,

$$\omega_1 = 2.0931947 \times 10^{-2} \text{ rad/s}$$

$$\omega_2 = 3.0404741 \times 10^{-2} \text{ rad/s}$$

$$\omega_3 = 3.9088122 \times 10^{-2} \text{ rad/s}$$

The uncontrolled motion of the linear system through small-amplitude deviations with respect to each of the three nominal orientations will now be considered.

Case 1: $I_x = I_y$ and $I_z = 2I_x = 2I_y$

The rotational equations of motion and the generic modal equations are nondimensionalized by the orbital period and the length variable ($\tau = \omega_c t$, $Z_r = A_r/a$, $\phi' = d\phi/d\tau$, etc.):

$$\psi'' = [(I_y - I_z - I_x)/\omega_c I_x]\phi' - [(I_y - I_z)/I_x]\psi \tag{9}$$

$$\phi'' = [(I_x - I_y + I_z)/\omega_c I_z]\psi' + 4[(I_x - I_y)/I_z]\phi \tag{10}$$

$$\theta'' = -3\theta \tag{11}$$

The generic mode equations become

$$Z_r'' = -(\omega_r/\omega_c)^2 Z_r \tag{12}$$

The pitch and the generic mode equations are decoupled from roll and yaw. The pitch and generic modes exhibit simple harmonic motions. After substituting inertia values into the roll and yaw equations, the roll-yaw system characteristic equation is developed and has a double pole at the origin. Thus, the uncontrolled roll-yaw motion for this example is unstable.

Case 2: $I_y = I_z$ and $I_x = 2I_y$

The rotational equations of motion are

$$\psi'' = -(1/\omega_c)\phi' \tag{13}$$

$$\phi'' = (2/\omega_c)\psi' + 4\phi \tag{14}$$

$$\theta'' = 3\theta \tag{15}$$

The generic mode equations can be represented by

$$Z_r'' = -[(\omega_r/\omega_c)^2 - 3]Z_r \tag{16}$$

From Eq. (15) the pitch amplitude increases exponentially in response to an initial displacement, whereas from Eq. (16), for $\omega_r/\omega_c > \sqrt{3}$ the generic modal amplitudes exhibit simple harmonic motion. The characteristic equation for the roll-yaw system, as in the previous case, has a double pole at the origin.

Cases 1 and 2 are specific examples of classic gravity-gradient instabilities previously shown by other authors for the case of uncontrolled motion.

Case 3: $I_x = I_z$ and $I_y = 2I_x = 2I_z$

The rotational equations of motion are

$$\psi'' = -\Psi \qquad \phi'' = -4\phi \qquad \theta'' = 0 \tag{17}$$

while the generic mode equations can be expressed by

$$Z_r'' = -[(\omega_r/\omega_c)^2 - 1]Z_r \tag{18}$$

In this case, roll, yaw, pitch, and the generic modes are decoupled from each other. The generic modes, roll, and yaw exhibit simple harmonic motion, while the pitch amplitude increases linearly with time for a given initial pitch rate.

For the more general case of large-amplitude rigid modes and large, flexural deformations, it should be noted that a completely nonlinear model for the system dynamics should be examined.

IV. Controlled Motion

The rotational equations of motion are combined with the generic modal equations using the nondimensional orbital time and length variables and then recast into conventional state space form:

$$X' = AX + BU \tag{19}$$

where the state vector X is defined as

$$X = (x_1, x_2, x_3, \ldots, x_{i+3}, \ldots\ldots, x_{n+6+i}, \ldots, x_{2n+6})^T$$

and

$$x_1 = \phi,\ x_2 = \psi,\ x_3 = \theta,\ x_{i+3} = Z_i = A_i/a$$

$$(i = 1,2,\ldots,n \text{ generic modes})$$

$$x_{n+4} = \phi',\ x_{n+5} = \psi',\ x_{n+6} = \theta',\ x_{n+6+i} = Z_i' = x_{i+3}'$$

$$(i = 1,2,\ldots,n)$$

For the examples to be considered in this paper it is assumed that the system can be modeled by three rigid-body rotational modes and the first three generic (flexible) modes.

The general A matrix

$$[A] = \left[\begin{array}{c|ccc} \text{null}_{6\times 6} & [I]_{6\times 6} & & \\ \hline \text{diagonal} & 0 & A_{78} & \ldots\ 0 \\ A_{6\times 6} & A_{78} & 0 & \ldots\ 0 \\ & \cdot & \cdot & \cdot\ \cdot \\ & \cdot & \cdot & \cdot\ \cdot \\ & 0 & 0 & \ldots\ 0 \end{array}\right] \tag{20}$$

The nonzero and nonunity elements appearing in A are

$$A_{7,1} = 4(I_x - I_y)/I_z \qquad A_{8,2} = -(I_y - I_z)/I_x$$

$$A_{9,3} = 3(I_x - I_z)/I_y \qquad A_{10,4} = -(\omega_1/\omega_c)^2$$

$$A_{11,5} = -(\omega_2/\omega_c)^2 \qquad A_{12,6} = -(\omega_3/\omega_c)^2$$

$$A_{8,7} = (I_y - I_z - I_x)/\omega_c I_x \qquad A_{7,8} = (I_x - I_y + I_z)/\omega_c I_z$$

for $\omega_i/\omega_c \gg 1$.

The general B matrix:

$$B=\left[\frac{\text{null}_{6\times 6}}{B_{6\times 6}}\right]$$

where the lower part of the B matrix depends on actuator locations.

Control laws are developed using four different techniques. They are: 1) decoupling of the original state equations using state variable feedback; 2) stabilizing the system by clustering the poles on a line parallel to the imaginary axis and in the negative s-plane using the control law of the type $U=-KX$; 3) applying the linear regulator theory to the original system equations; and 4) command control by complete decoupling. For all cases, controllability has been verified for a given placement of actuators using a numerical algorithm.[8] The mass and inertia properties of the plate previously assumed for the uncontrolled motion will also be used for the study of the controlled motion.

The four techniques selected for determining control laws approach this problem from different points of view. In the case of decoupling techniques, the individual behavior of the original coordinates is emphasized (as contrasted to that of a transformed modal set); in the pole clustering method, the overall transient requirements of the system are considered instead of concentrating on the behavior of the individual coordinates; the linear regulator theory provides for the a priori setting of penalty weighting functions on the control effort as well as on the state variables; finally, the command control by decoupling is useful when it is desired to control the spacecraft shape and/or orientation in a particular direction without disturbing the other components of the state. A comparison of the results obtained using these techniques should give insight into a range of control forces and settling times required in accordance with the various control objectives.

A. Decoupling of Original State Equations Using State Variable Feedback

The equations of motion of the platform can be written as

$$\ddot{X}=A\dot{X}+CX+BU \tag{21}$$

where $X=(x_1,x_2,\ldots,x_{n+3})$. After selecting $U=K_r\dot{X}+K_pX$, we can rewrite the controlled motion equations as

$$\ddot{X}=(A+BK_r)\dot{X}+(C+BK_p)X \tag{22}$$

where K_r and K_p are evaluated such that $(A+BK_r)$ and $(C+BK_p)$ are diagonalized and thus yield required damping and frequency of the controlled modes. The number of modes must be equal to the number of actuators to avoid the use of pseudoinverse matrices.

Two sets of actuator locations have been assumed for each of the three nominal orientations previously described. For all orientations (cases 1-3) it is assumed that five actuators are located on the larger surface (with force axis normal to it) and a sixth actuator along an edge. Actuator positions for the two different sets of locations are illustrated in Fig. 2, represented by locations I and II, respectively. The system A matrices corresponding to the three nominal orientations are listed as follows:

Case 1: The nonzero elements of the A matrix are $A_{i,i+6}=1$ for $i=1,\ldots,6$; $A_{7,8}=800$; $A_{8,7}=-1600$; $A_{8,2}=1$; $A_{9,3}=-3$; $A_{10,4}=-277.414$; $A_{11,5}=-588.647$; $A_{12,6}=-976.844$.

Case 2: The elements of the A matrix that are different from case 1 are $A_{7,1}=4$; $A_{7,8}=1600$; $A_{8,2}=0$; $A_{8,7}=-800$; $A_{9,3}=3$.

Case 3: The elements of the A matrix that are different from case 1 are $A_{7,1}=-4$; $A_{7,8}=0$; $A_{8,2}=-1$; $A_{8,7}=0$; $A_{9,3}=0$.

As an example, the nontrivial part of the B matrix for case 3 is calculated as shown in Table 1. For the other two nominal orientations the elements of the B matrix are given in Ref. 7. For all combinations considered above the gains are selected in order to produce 20% of critical damping in each of the rigid body modes and the first generic mode, and 10% of critical damping in the second and third generic modes. In order to provide a better transient response in the lower-frequency fundamental elastic mode, the percentage of critical damping is selected to be twice that in the remaining flexible modes. The time response of the rigid body modes and the generic modal amplitudes for all combinations considered and for equal initial position displacements in all components of the state is illustrated in Fig. 3a.

As an example of the time history of the required control forces, Fig. 3b shows such a time response for the exterior location (II) of the actuators with the platform nominally following the local vertical and the major surface area of the platform in the orbital plane. A complete summary of the maximum force amplitudes required for all combinations of actuator locations and platform orientations is given in Table 2. In interpreting the results of Table 2, it should be pointed out that in the process of achieving both orientation and shape control, the maximum force(s) required of any actuator will vary with both the moment arm about the principal body axes and the value of the modal shape function at the particular actuator location for all modes contained within the mathematical model.

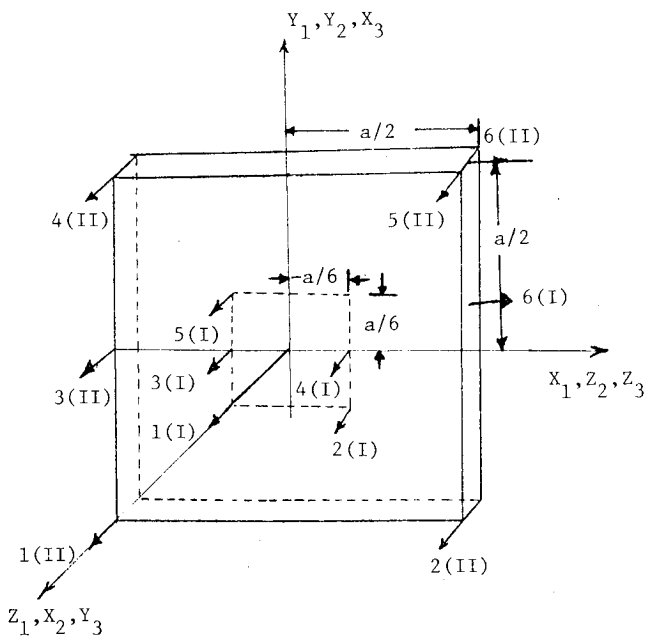

Fig. 2 Locations (I and II) of two sets of actuators. Coordinate axes: case 1—$X_1Y_1Z_1$; case 2—$X_2Y_2Z_2$; case 3—$X_3Y_3Z_3$. $a=100$ m

B. Stabilizing the System by Pole Clustering

The equations of motion of the platform when recast in state space format can be written as

$$\dot{X}=AX+BU \qquad X\to 2(n+3)\times 1 \tag{23}$$

The control, $U=-KX$ is selected by using a digital computer algorithm[8] such that $(A-BK)$ has the required identical negative real part in each of its eigenvalues. Although the number of actuators can be less than the number of modes (one half of the dimensionality of the state vector), a limitation of this algorithm is that the gains are selected such that all of the closed-loop poles lie on a line parallel to the

Table 1 Lower part of control influence matrix—case 3

Location I (lower part of B matrix)					
−0.4529	−0.4529	0.0	0.0	0.4529	0.0
0.4529	−0.4529	−0.4529	−0.4529	0.4529	0.0
0.0	0.0	0.0	0.0	0.0	−0.22645
0.003126	−0.003126	0.0	0.0	−0.003126	0.0
0.0	0.0	−0.0030844	−0.0030844	0.0	0.0
−0.008786	−0.008786	−0.0115	−0.0115	−0.008786	0.0
Location II (lower part of B matrix)					
−1.3592	−1.3592	1.3592	1.3592	0.0	0.0
1.3592	−1.3592	1.3592	−1.3592	1.3592	0.0
0.0	0.0	0.0	0.0	0.0	−0.6796
0.023	−0.023	−0.023	0.023	0.0	0.0
0.0	0.0	0.0	0.0	−0.023	0.0
0.023	0.023	0.023	0.023	0.023	0.0

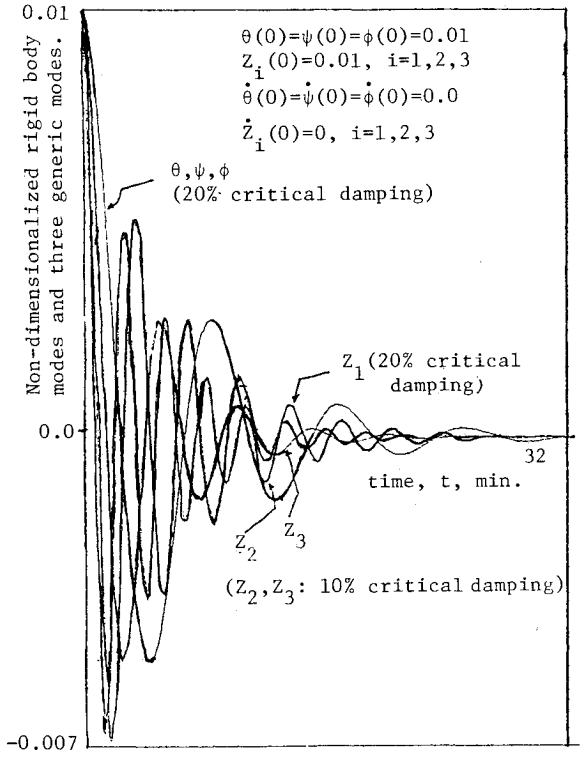

Fig. 3a Controlled state response for all combinations of orientations and actuator locations.

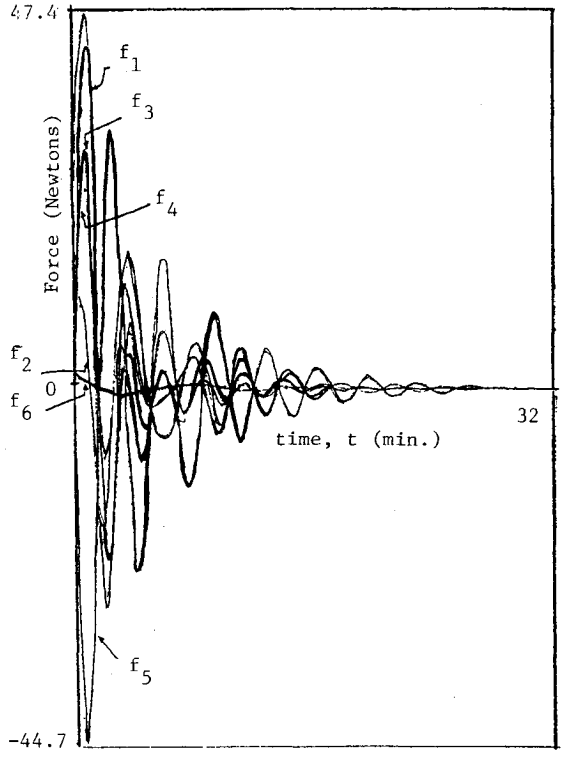

Fig. 3b Control force time history for case 3 at location II.

imaginary axis. This algorithm is useful, however, when it is important that each mode in the system satisfy some minimum damping characteristics.

As an example of this technique, we consider the system with four actuators and six modes where control about the first orientation (case 1) is desired. Three of the actuators are assumed to provide forces perpendicular to the major surface with the remaining actuator thrusting normal to an edge. The actuator coordinates in the body system (Fig. 1a) are: $f_1(-a/6, -a/6, 0)$; $f_2(a/6, -a/6, 0)$; $f_3(-a/6, 0, 0)$; and $f_4(a/2, a/6, 0)$, where $a = 100$ m. It is assumed that the minimum damping requirement on the system has a time constant of 13.33 min (or $\frac{1}{2}\pi$-dimensional orbital time). The control influence matrix is then calculated based on the assumed coordinates of the four actuators. The control $U = -KX$ can be calculated by the ORACLS pole clustering algorithm. Based on these gains, time histories of the required control forces are then obtained.

The control influence matrix (lower part), closed-loop poles, and maximum-force amplitudes required are summarized as follows:

B matrix (lower part) =

$$\begin{bmatrix} 0.0 & 0.0 & 0.0 & -0.22645 \\ -0.4529 & -0.4529 & 0.0 & 0.0 \\ 0.4529 & -0.4529 & 0.0 & 0.0 \\ 0.003126 & -0.003126 & 0.0 & 0.0 \\ 0.0 & 0.0 & -0.0030844 & 0.0 \\ -0.008786 & -0.008786 & -0.0115 & 0.0 \end{bmatrix}$$

The real part of the closed-loop poles (nondimensionalized) is -1.0 and the imaginary parts are ± 0.000485, ± 0.993, ± 16.82, ± 24.26, ± 31.33, and ± 1131.37.

The maximum force amplitudes (Newtons) are calculated as $|f_1| = 78.5$, $|f_2| = 36.4$, $|f_3| = 169.5$, and $|f_4| = 35.3$.

Table 2 Maximum force amplitudes (newtons) for different combinations of cases with actuator locations[a]

	Location I (interior)			Location II (exterior)		
Force	Case 1	Case 2	Case 3	Case 1	Case 2	Case 3
f_1	−807.8	270.63	270.6	57.6	62.56	47.4
f_2	270.0	−136.2	−133.3	28.19	26.20	−17.2
f_3	1141.0	387.3	−425.0	−65.89	−49.5	30.0
f_4	527.9	195.6	163.7	17.10	−30.90	25.08
f_5	489.09	−253.3	153.0	−44.6	−44.67	−44.67
f_6	−264.58	−272.0	4.4	88.16	−88.06	1.47

[a] Underscore indicates maximum level of control force required for each case.

An interesting comparison can now be made between this result and that shown in Table 2 for case 1 and the first location (I) of the six actuators considered there. It can be seen that by using fewer actuators, appropriately placed, that better transient response characteristics can be obtained with smaller maximum-force amplitudes. However, a disadvantage of this method is that some of the controlled frequencies may be orders of magnitude greater than the highest frequency of the uncontrolled system (for this example, compare 1131 with $\sqrt{976} = 31.24$). Depending on the nature of the expected disturbance forces, this result could be very undesirable.

C. Application of the Linear Regulator Theory

The control law, $U = -KX$, is selected such that the following performance index is minimized

$$J = \int_0^\infty (X^T Q X + U^T R U)\,dt \tag{24}$$

where Q and R are positive-definite penalty matrices. The steady-state solution of the matrix Riccati equation of dimension equal to the state has to be solved in order to evaluate the gain matrix, K.

A computer algorithm within the ORACLS[8] software package is used to obtain the gain matrices, K, for different combinations of the Q and R penalty matrices. This algorithm utilizes the Newton-Raphson method of solving the Ricatti equation. In the examples considered here, four actuators are assumed with the system represented by three rigid-body and three flexible modes. The locations of the four actuators are taken to be the same as in Sec. IV. B and control about the first nominal orientation (case 1) is considered.

The weighting matrix, Q, is selected based on the following considerations. For the example considered here, it can be seen from Eqs. (19) and (20), and the B matrix that the uncontrolled system dynamics is either described by sets of uncoupled harmonic oscillators, or, in the case of roll/yaw motion, by a coupled two-dimensional harmonic oscillator. The latter motion can be represented by

$$\begin{bmatrix} \omega_z' \\ \omega_x' \end{bmatrix} = \begin{bmatrix} 0 & a \\ -b & 0 \end{bmatrix} \begin{bmatrix} \omega_z \\ \omega_x \end{bmatrix} \tag{25}$$

where the system oscillates at the frequency $\Omega = \sqrt{ab}$. It is desired that the control remove a maximum "transverse" angular rate,

$$\omega_{T_{\max}} = \max\sqrt{\omega_z^2 + \omega_x^2} = \sqrt{\omega_z^2(0) + \omega_x^2(0)}$$

so that a strategy for selecting the elements of Q could be[9,10]

$$Q = \begin{bmatrix} f & 0 \\ 0 & f \end{bmatrix} \tag{26}$$

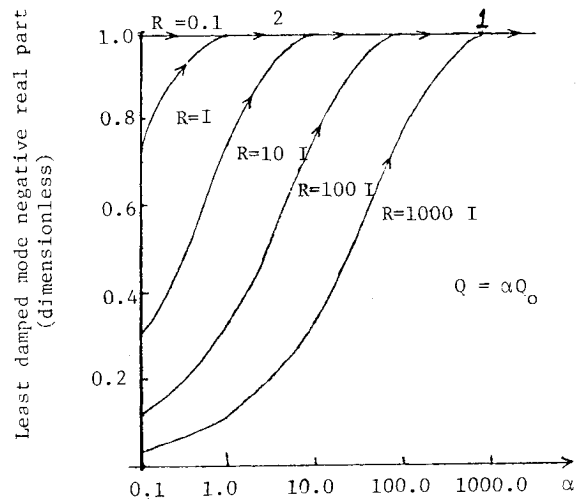

Fig. 4 Variation of least damped mode negative real part with α, R.

where $f = \Omega^2/\omega_{T_{\max}}^2$ when the control penalty matrix is fixed. The remaining equations for any of the uncoupled oscillators can also be expressed by

$$\begin{bmatrix} z_i' \\ z_i'' \end{bmatrix} = \begin{bmatrix} 0 & 1 \\ -(\omega_i/\omega_c)^2 & 0 \end{bmatrix} \begin{bmatrix} z_i \\ z_i' \end{bmatrix} \tag{27}$$

in the same format as Eq. (25), and thus the weights can be obtained in a similar manner.

The Q matrix for the case considered here [control about nominal orientation (case 1) with actuator locations as given in Sec. IV. B] is obtained using the relations given by Eq. (26) and is a diagonal matrix, Q_0, with the following elements: $Q_{1,1} = 4.32 \times 10^9$, $Q_{2,2} = 8.539 \times 10^9$, $Q_{3,3} = Q_{9,9} = 3.0 \times 10^4$, $Q_{4,4} = Q_{10,10} = 2.77414 \times 10^6$, $Q_{5,5} = Q_{11,11} = 5.88647 \times 10^6$, $Q_{6,6} = Q_{12,12} = 9.74844 \times 10^6$, $Q_{7,7} = Q_{8,8} = 2.222 \times 10^3$.

The R_0 matrix is chosen as an identity matrix. A parametric study is done using various multiples of the Q_0 ($Q = \alpha Q_0$) and R_0 matrices obtained above which are plotted against the negative real part of the least-damped mode of the controlled system in Fig. 4. All the loci of the negative real part of the least-damped mode approach unity and no significant improvement is observed by increasing the state penalty $Q = \alpha Q_0$ any further. Thus, one wishes to operate on the horizontal line between points 1 and 2. The maximum amplitude of the forces for $R = I$ and $R = 1000\ I$ are calculated and plotted in Fig. 5. The closed-loop poles of the controlled system at points 1 and 2 are virtually the same and are given as follows (nondimensionalized): -1.0043, $-1.8 \pm i16.64$, $-2.16 \pm i24.20$, $-17.18 \pm i19.79$, -26.23, -36.22, -137.64, and $-38.66 \pm i1132.11$.

The maximum force amplitudes as shown in Fig. 5 are less than those corresponding to case 1, location I of Table 2 for comparable transient responses, whereas these are high as

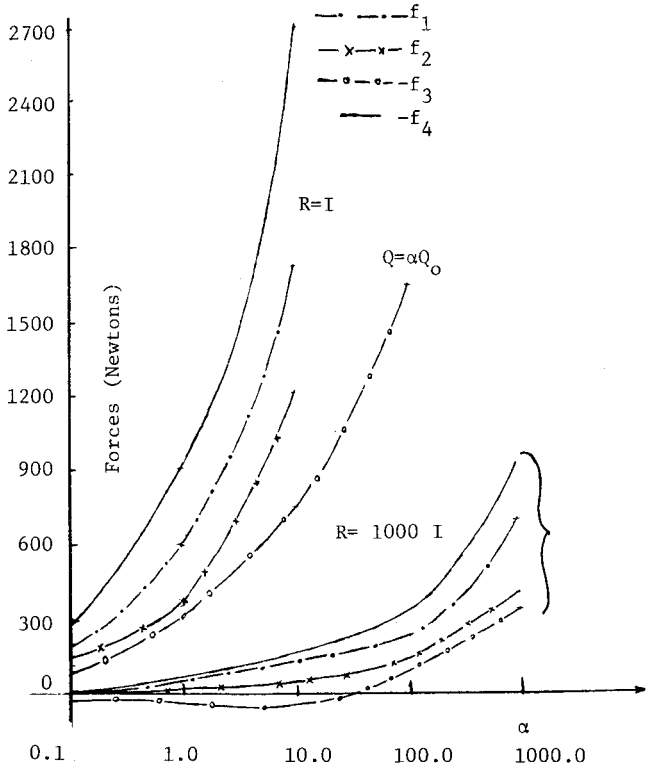

Fig. 5 Maximum force amplitudes as a function of α and Q for all actuators (application of linear regulator theory).

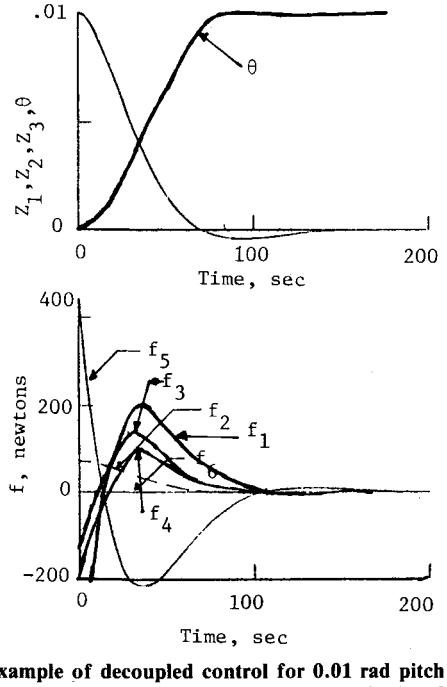

Fig. 6 Example of decoupled control for 0.01 rad pitch command combined with zero modal-amplitude commands ($\omega = 0.05$ rad/s, $\zeta = 0.7$) for case 1 at location II.

compared to the forces obtained using the pole-clustering technique. This is due to the large negative real part (−1.0). Both the linear regulator and pole-clustering technique have the drawback that the controlled frequencies can be quite high compared to the uncontrolled frequencies.

These higher (controlled) frequencies may correspond to the frequencies of higher-order modes not contained in the previously truncated system model. In order to completely consider such effects the order of the original system model would have to be greatly expanded in order to avoid the possible effects of control spillover (not considered in the present analysis). On the other hand, these techniques have the advantage that they can be applied to situations where the number of actuators is less than the number of modes in the mathematical model, in contrast to the decoupling technique of Sec. IV. A.

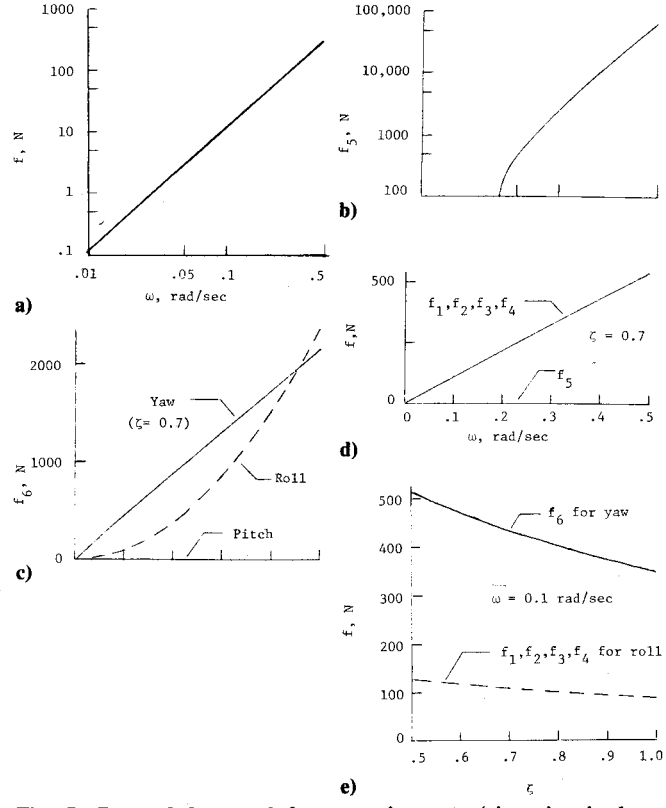

Fig. 7 Decoupled control force requirements (given in absolute values) for roll, yaw, and pitch commands of 0.01 rad: a) requirements of first four actuators for pitch or yaw commands; b) maximum requirements for pitch command combined with zero commands for disturbances of 1.0 m in the modal amplitudes; c) requirements of sixth actuator for roll, yaw, and pitch commands; d) requirements of first five actuators for roll command; e) effect of damping on requirements.

D. Command Control by Complete Decoupling

The control law $u = Fx + Gv$ is selected such that the feedback gains, F, and the feedforward gains, G, provide independent control for each of the rigid-body and flexible modes for any specified command v.[6] The G-gain matrix is the inverse of the control-influence matrix, B, and operates on the command inputs. The F gains operate on the measurements of all the states and can be adjusted to provide desired closed-loop dynamics (angular frequency, ω, and damping factor, ζ) for the overall system without destroying the decoupling process. Values of ω and ζ can be arbitrarily selected for each of the rigid-body and flexible modes.

An example of this decoupling technique is shown in Fig. 6 for a combined command wherein a change of 0.01 rad in pitch attitude is required along with the nulling of 1-m disturbances in each of the three flexible modes. The results correspond to the case of complete decoupling, in that the number of control actuators equals the number of modes in the model. The decoupling technique can be applied, however, to the case wherein the number of actuators is reduced, without destroying the overall control of the system.[11]

The time histories in Fig. 6 depict the responses of the rigid-body and flexible modes, caused by instantaneous step commands along with the resulting actuator-force requirements. The closed-loop dynamics selected for this case

were $\omega = 0.05$ rad/s and $\zeta = 0.7$ for all rigid-body and flexible modes. The plot shows that the pitch-attitude and flexible-mode responses reach equilibrium after about 100 s and the roll and yaw responses are unaffected, as required. The maximum force requirements of about 450 N are seen to occur for actuators f_1 and f_5.

A parametric plot of maximum control-force requirements is presented in Fig. 7 for a range of closed-loop dynamics, ω and ζ. This figure represents data for a complete decoupling process; therefore, the results should be considered as the ideal case, inasmuch as there are no effects due to control spillover (effect of fewer number of actuators than modes) or observation spillover (effect of unmodeled modes on the measurements). As shown by Fig. 7e, the damping factor ζ only affects f_6 for yaw commands and the first four actuators for roll commands. The control forces in Fig. 7e occur after the initial time ($t = 0$) and the effects of ζ are seen to be relatively small in comparison to the effects of ω (see, for example, the effect of ω on f_6 for yaw in Fig. 7c). It is interesting to note from Fig. 7b that the control-force requirements for the zero commands in nulling the flexible-mode disturbances of 1 m are considerably higher than the requirements for the individual attitude commands. For Fig. 7b it should be noted that, for values of ω below about 0.04 rad/s, the control forces change sign; however, the magnitudes of the forces remain within the range of hundreds of newtons.

V. Conclusions

In this paper, the dynamics, stability, and control of an orbiting homogeneous, flexible square platform are considered. Three different nominal orientations of the platform are examined. When the platform is nominally following the local vertical with its larger surface perpendicular to the orbital plane and when the platform follows the local horizontal with its larger surface normal to the local vertical, it is seen that the uncontrolled roll/yaw motion is unstable. For the case where the platform follows the local vertical with its large surface perpendicular to the orbit normal, the uncontrolled pitch motion is found to be unstable.

Four different control techniques are considered for the selection of the control laws:

1) The decoupling of the original state equations using state variable feedback eliminates the need of a transformation from the original coordinates to the modal coordinates and provides a method of directly specifying the amount of damping and frequency of the individual components of the state vector. However, with this technique, the number of actuators must be equal to the number of coordinates (modes) in the model.

2) The pole placement algorithm (ORACLS) guarantees the overall required damping of the system and does not restrict the number of actuators to be equal to the number of modes in the model. However, it is seen that the closed-loop frequencies may be greatly increased when compared to the open-loop values which may cause problems with externally induced periodic excitations.

3) The linear regulator theory can provide acceptable performance once the state and penalty matrices are properly selected, and the number of actuators can be less than the number of modes in the model. Computer capacity and accuracy limit the number of modes that can be considered. Here, too, an increase in the closed-loop frequencies may result in order to provide satisfactory responses with maximum allowable force amplitudes.

4) The command control technique allows one to change one (or more) components of the state vector to a different nominal value without disturbing the other components. Also, as in the case for the first three techniques (which are applied to control the state about the original equilibrium orientation), the command technique provides control for nulling external disturbances on the system. The technique covers a wide range of values selected for the closed-loop dynamics, showing the drastic effect of closed-loop frequency on the control force requirement.

Acknowledgments

This research was partially supported by NASA Grant NSG-1414, Supplement 2.

References

[1] "Outlook for Space," NASA Rept. SP-386, Jan. 1976.

[2] "Industry Workshop on Large Space Structures," NASA Contractor Rept. CR-2709, Contract No. NAS-1-12436 for NASA Langley Research Center, May 1976.

[3] Kumar, V.K. and Bainum, P.M., "Dynamics of a Flexible Body in Orbit," AIAA Paper 78-1418, Aug. 1978; also, *Journal of Guidance and Control,* Vol. 3, Jan.-Feb. 1980, pp. 90-92.

[4] Santini, P., "Stability of Flexible Spacecrafts," *Acta Astronautica,* Vol. 3, 1977, pp. 685-713.

[5] Bainum, P.M. and Reddy, A.S.S.R., "On the Controllability of a Long Flexible Beam in Orbit," *Proceedings of the Second AIAA Symposium on Dynamics and Control of Large Flexible Spacecraft,* June 1979, edited by L. Meirovitch, VPI & SU Press, 1980, pp. 145-159.

[6] Reddy, A.S.S.R., Bainum, P.M., and Hamer, H.A., "Decoupling Control of a Long Flexible Beam in Orbit," *Astrodynamics 1979, Advances in the Astronautical Sciences,* Vol. 40, Pt. II, AAS Publication, 1980, pp. 649-673.

[7] Bainum, P.M., Reddy, A.S.S.R., Krishna, R., and James, P., "The Dynamics and Control of Large Flexible Space Structures III," Final Report, NASA Grant NSG-1414, Supplement 2, Part A: Shape and Orientation Control of a Platform in Orbit using Point Actuators, Howard University, June 1980.

[8] Armstrong, E.S., "ORACLS—A System for Linear-Quadratic-Gaussian Control Law Design," NASA TP 1106, April 1978.

[9] Bainum, P.M. and Sellappan, R., "Optimal Control of Spin-Stabilized Spacecraft with Telescoping Appendages," *The Journal of the Astronautical Sciences,* Vol. XXIV, Oct.-Dec. 1976, pp. 329-346.

[10] Amieux, J.C. and Liegeois, A., "Design and Ground Test of a Pendulum-Type Active Nutation Damper," *Journal of Spacecraft and Rockets,* Vol. 11, Nov. 1974, pp. 790-792.

[11] Hamer, H.A. and Johnson, K.G., "Decoupled Control of a Long Flexible Beam in Orbit," NASA TP 1740, Dec. 1980.